

Highlights

Multi-Objective Multidisciplinary Optimization of Wave Energy Converter Array Layout and Controls

Kapil Khanal^a, Nate DeGoede^b, Olivia Vitale^b, Maha N. Haji^{a,b}

- Optimal designs differ by 37% in ocean space used and 5% in LCOE.
- The q-factor for optimal designs range between 1 and 1.06
- Optimal configurations for 4 heaving WECs is rhombus-like shape
- Regression model interprets the trade-off between objectives for optimal designs
- Sensitivity analysis suggests mild sensitivity to wave environment and interest rate

Multi-Objective Multidisciplinary Optimization of Wave Energy Converter Array Layout and Controls

Kapil Khanal^a, Nate DeGoede^b, Olivia Vitale^b, Maha N. Haji^{a,b}

^a*Systems Engineering, Cornell University, Ithaca, NY, USA*

^b*Mechanical and Aerospace Engineering, Cornell University, Ithaca, NY, USA*

Abstract

This study utilizes multidisciplinary design optimization (MDO) to design an array of heaving wave energy converters (WECs) for grid-scale energy production with decision variables and parameters chosen from the coupled disciplines of geometry, hydrodynamics, layout, motor-actuated reactive controls (with a force maximum constraint) and economics. We vary a WEC's dimensions, array layout, and control gain to minimize two objectives: the levelized cost of energy (LCOE) and the maximum separation distance. This multi-objective optimization approach results in a set of optimal design configurations that stakeholders can choose from for their specific application and needs. The framework yields a range of optimal (minimum) LCOE values from 0.21 to 0.23 \$/kWh and a separation distance ranging from 97 to 62 meters. The WEC radius of 4m is found to be optimal, and the q-factor for optimal designs are greater than 1 up to 1.06. The optimal configuration for 4 heaving WECs is found to be a rhombus-like layout. Additionally, a post-optimality global sensitivity analysis is performed to analyze the interaction of several parameters. The uncertainty (variance) of the LCOE is quantified in terms of the uncertainty of the input parameters and interpreted to aid in decision making. Wave heading, wave frequency, WEC lifetime, amplitude and interest rate accounts for most of the variance in the optimal LCOE configuration. Different designs in the Pareto set may be appealing for different decision makers based on their trade-off analysis. To that end, an ad-hoc regression model is developed for trade-off analysis between objectives and some design heuristics are provided.

Keywords: Multidisciplinary WEC Layout optimization, Genetic Algorithm, Pareto Optimal Design, Global Sensitivity Analysis, Design Heuristics

1. Introduction

Wave energy converters (WECs) convert the oscillatory motion of ocean waves into usable mechanical or electrical energy (Budal, 1977a). Multiple WECs are required at a site for grid scale integration, motivating the study of WEC arrays, or farms. Wave farms have the potential to supply 34% of the US electric supply needs (Kilcher et al., 2021). However, implementing these offshore systems is expensive and challenging. Aside from the bureaucratic and permitting hurdles that exist for developing WEC farms outlined in the study by Freeman et al. (2022), many technical challenges still face the industry. Babarit et al detailed the “park effect” of WEC arrays, where the waves radiated and diffracted from each body affect the motion of all interacting bodies, thereby affecting total farm power output (Babarit, 2013). Designing a farm configuration that increases power output requires detailed numerical models that account for these interactions. Computational expenses for the numerical solver scales cubically with the number of WEC bodies, making numerical hydrodynamic modeling difficult for large arrays (Newman, 1985). Several modeling methods exist for various types of array investigations (Folley et al. (2012), Yang et al. (2022)), but there is no universally applicable model. Numerical solutions along with a series of design studies for the trade-off analysis between competing objectives are necessary for WEC farms.

When optimizing WEC arrays, the number of WECs, separation distance, array layout, and wave environment are shown to be important factors for WEC farms (de Andrés et al. (2014)) and thus must be included in early design studies. Bozzi et al. (2017) simulated WEC array configurations in real-wave conditions off the Italian coastline. They highlighted the importance of dominant wave heading on determining the optimal configuration; however, the optimal designs found were based on brute-force optimization for maximizing power using only four configurations. Lyu et al. (2019) used a genetic algorithm to optimize 3, 5, and 7-body arrays for configuration and body dimension, finding up to a 39% increase in power production when optimizing both design variables. They also emphasize that the control method influences the optimal array. However, their optimal designs include WECs of the same architecture with slightly different radii and drafts, making the design impractical from an economics of scale standpoint. Most models in lit-

erature optimize solely for power production (Babarit et al., 2012),(Götteman et al., 2015),(Abdulkadir and Abdelkhalik, 2023), ignoring other maritime priorities.

Marine spatial planning (MSP) is an important factor when attempting marine developments. Managing space for all maritime markets (fishing, renewable energy, marine conservation, shipping routes, etc.) is required when creating offshore developments (Ehler (2021)). It is also imperative to keep WECs within an optimal siting location because of ecological considerations such as disturbances, noise and many ecosystem elements (Galparsoro et al. (2021)). Ensuring the farm can be practically sited and coexist with other maritime markets is essential for their successful real-world implementation. The siting location and ocean space required is influenced by the distances between the WECs in a farm. Many studies find a distance as a function of WEC diameter where bodies should be placed to avoid interactions (Bozzi et al. (2017), Babarit (2013), Singh and Babarit (2014)). However, these distances are large (greater than 10 times the WEC diameter) and may be impractical for arrays from an operation, maintenance and mooring infrastructure development point of view. Thus, exploiting array effects in compact configurations is crucial for bringing WEC farms to fruition.

This optimization study analyzes economic viability, ocean space used, and power production for a 4-body WEC farm in regular waves. Economics are reported through the levelized cost of energy (LCOE), which measures the cost of energy production over the lifetime of the system and provides a benchmark for cost comparison (Nahvi and Ali (2018)). The ocean space used is characterized by the farm length; the maximum distance between any two WECs. LCOE and farm length are both minimized in the optimization. For additional analysis (not directly optimized), the power production for the optimal designs is also reported in terms of q-factor. Q-factor is a metric used to compare the total power production of an n -body array to the power production of n isolated WECs. These objectives depend on WEC geometry and layout, hydrodynamics, controls, and economics. All these disciplines rely on each other, making this a high dimensional multidisciplinary system design problem. Individual WECs have been already designed in multidisciplinary way (McCabe et al., 2022). This study introduces the application of the MDO technique to the array layout optimization. Such a formulation is considered to provide better designs than conventional sequential design optimization (Martins and Ning, 2022).

In addition to the optimization, a sensitivity study to explore the inter-

action of the parameters between different technical disciplines is of vital importance. Understanding these relationships is not just a mathematical problem but also will help accelerate adoption and permitting of engineered systems. A study conducted at the PacWave wave energy test facility found that addressing uncertainty regarding wave technologies is one of several areas of utmost importance for the most stakeholders (Freeman et al., 2022). Similarly, a report by Sandia national lab points out that the WEC farms readiness has been too focused on commercial readiness and not enough on the stakeholder requirements and economic viability required for market entry (Roberts et al.). They document that among many requirements for successful wave energy farms, it is essential that they are economically competitive and address social considerations. In this paper, a global sensitivity analysis (GSA) is conducted for the sensitivity calculation to the optimal result from optimization study with many objectives, coming from different stakeholders. This technique captures the global behaviour of the models and has been applied to many engineering systems such as wind farms (Carta et al., 2020).

Uncertain ocean parameters affect the power production of a WEC, and should therefore be quantified as they provide valuable information on location data and the expected variability of the power production. Metrics like LCOE are sensitive to environmental, dynamic and economic parameters. Various authors have looked into the local variation of these metrics to quantify their performance. Sinha et al. (2016) investigated the influence of incident angle on the power absorption and power consistency of different fixed optimally tuned array configurations. They found that for concentric and circular arrays, the power absorption profile remains the same while for linear and grid type arrays, the power absorption increases with increase in incident from 0 to 90 degrees suggesting sensitivity of incidence angle on array configurations. Sharp and DuPont (2018) performed a minimum separation study and quantified the significance of the the separating distance on array performance metrics. Different restrictions on the distance resulted in different layouts. This could be partly attributed to simpler model (McNatt et al., 2015) they used for the hydrodynamic calculations. Using a more accurate hydrodynamic model may provide more insight into its interactions with other disciplines and the design space becomes much 'richer' for the power calculations. For example, interaction between wave environment and economics parameters are lacking in most of these studies. Similarly, rather than solely performing limited local parameter studies on a few common

configurations, it is essential to integrate sensitivity analysis with the layout optimization studies within a complete multidisciplinary model of the WEC farms, as considered in this paper.

A global sensitivity analysis based on Sobol indices and variance decomposition (Saltelli et al., 1993) is used to calculate the sensitivity of most important parameters for the recommended Pareto optimal design. A variance-based uncertainty quantification is used because it is model-independent and can capture global interactions between input parameters. This also means that this method can be coupled with other software frameworks for hydrodynamic and optimization analysis. Sensitivity analysis is performed for the recommended Pareto optimal design, partly due to complexity for the disciplinary analysis such as the numerical simulation. The curse of dimensionality prevents the use of this method within an optimization. The approach we take enhances the understanding of the Pareto designs by providing the sensitivities.

In Section 2, we discuss the simulation model, and optimization formulation, and Section 3 describes the validation of the hydrodynamic model. Section 4 discusses the results of the optimization, and Section 5 discusses the post-optimality sensitivity analysis, and Section 6 discusses the future work.

2. Methodology

In this section, we discuss the problem formulation and introduce a design structure matrix of the multidisciplinary model consisting of several modules. Each individual module and its coupling with other disciplines is discussed.

2.1. Problem Formulations

In standard MDO problem formulations, each discipline is modeled as a separate module. The overall problem includes one or more objectives and constraints with multiple design variables and parameters. The interdependency between disciplinary modules are shown via coupling variables which can result in both feedforward and feedback loops. A multidisciplinary feasibility (MDF) is then obtained for the coupled disciplines (Cramer et al., 1994). The formal MDO definition of the problem discussed in this paper is given by

$$\begin{aligned}
& \text{Minimize} && \begin{bmatrix} LCOE(\mathbf{x}, \mathbf{p}; \hat{u}) \\ SPACE_{\max}(\mathbf{x}, \mathbf{p}; \hat{u}) \end{bmatrix} \\
& \text{by varying} && \mathbf{x} \\
& \text{subject to} && C_0 = 5r - \sqrt{(x_i - x_j)^2 + (y_i - y_j)^2} \leq 0 \\
& \text{while solving} && R_i(\mathbf{x}, \mathbf{p}; \hat{u}) = 0 \\
& && \text{for } \hat{u}
\end{aligned}$$

where $LCOE$ and $SPACE_{\max}$ are the two objectives to be minimized, \mathbf{x} is the vector of design variables. r is the WEC radius (discretized in the increment of 0.5m), (x_i, y_i) and (x_j, y_j) are the WEC coordinates of which first WEC is always fixed at $(0, 0)$. The vector of the coupled variables is \hat{u} . R_i refers to the governing equations in any of the disciplines. Inequality constraint (C_0) ensures the WECs remain a distance of at least five times the radius apart. This value provides a large enough distance to prevent collisions between WECs, but also close enough that interactions between bodies will still affect the system in complex ways (Singh and Babarit, 2014).

A visualization of the space objective and constraint C_0 is show in Fig. 2 and Table 1 details the parameters, design variables, constraints, and objectives. The xDSM (Lambe and Martins, 2012) diagram (Fig. 1) depicts the simulation models, disciplines used, and their interactions. All coupling variables are either explicitly or implicitly the function of the design vectors. The disciplines are ordered to ensure that no feedback loops exist in the xDSM diagram.

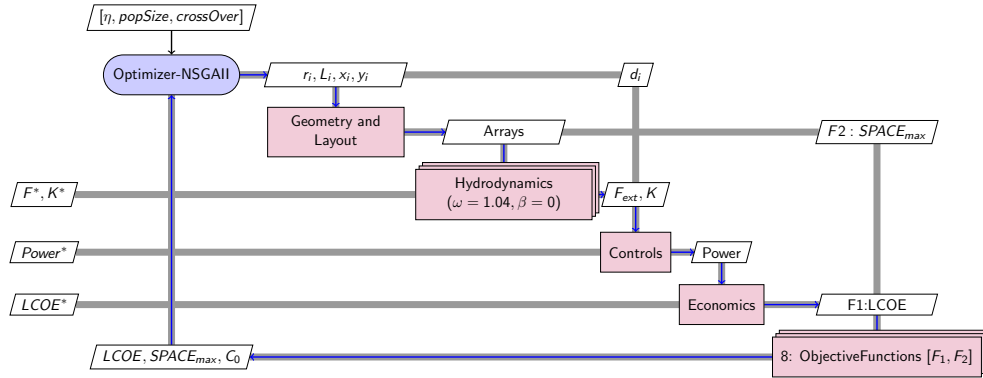


Figure 1: xDSM diagram of the multidisciplinary model of WEC farms. This architecture couples the optimizer with the multidisciplinary analysis of all the relevant modules. The diagonals are the disciplines and off-diagonals are the coupling variables. The input design variables are shown passing from the top and output of each discipline is shown on the right. The optimal value for each discipline is shown with an asterisk(*) of the left after the optimizer converges. The grey line shows the data I/O and blue line shows the sequence of analysis.

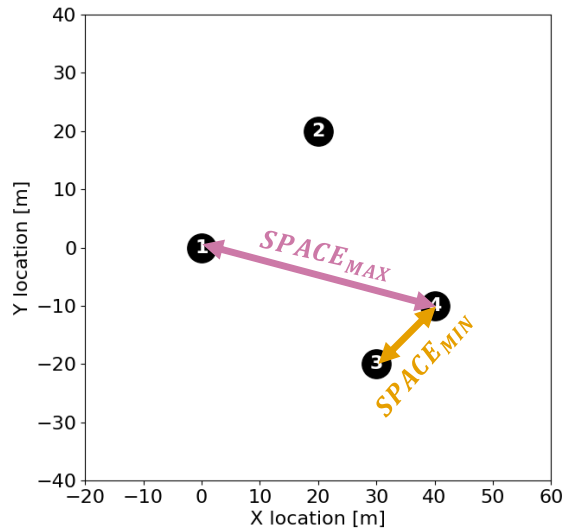


Figure 2: Plot showing the minimum space constraint and the $SPACE_{max}$ objective.

The input design vector is

$$\mathbf{x} = [2r, \ell/r, \log_{10}(d_1), x_2, y_2, \log_{10}(d_2), x_3, y_3, \log_{10}(d_3), \dots, x_n, y_n, \log_{10}(d_n)]^T \quad (1)$$

where ℓ is the length of the WEC, d is the damping of the power take-off system (PTO), and subscript n represents the total number of WECs. Fig. 3 shows the WEC geometry and control design variables. Also note that the design variable $2r$, representing diameter, is limited to integer values.

Table 1: Main Table outlining the parameters, design variables, constraint, and objectives in this MDO formulation.

	Name	Symbol	Notes
Parameters	Wave Frequency	ω	1.047 rad/s used in this study
	Wave Amplitude	A	1 m used in this study
	Wave Direction	β	measured from +x axis 0 rad used in this study
	Interest Rate	i	7%
	Wave Resource Availability	η_{avail}	95%
	WEC Life Span	L	25 years
	Array Scaling Factor	S	0.65
	PTO Force Maximum	F_{max}	2.6×10^5 N (optimum from Peña-Sanchez et al. (2022))
	Median Capital Cost	$CAPEX_{med}$	\$9000/kW
Design Variables	WEC Radius	r	ranges from 2 to 10 m
	WEC Length	ℓ	ranges from $0.1r$ to $2r$
	X Location	x_i	ranges from -500 m to 500 m x_1 is fixed at 0 m
	Y Location	y_i	ranges from -500 m to 500 m y_1 is fixed at 0
	PTO Damping	d_i	ranges from 1 to 10,000,000 Ns/m
Constraints	Minimum WEC Spacing	$SPACE_{min}$	must be larger than $5r$
Objectives	Levelized Cost of Energy	$LCOE$	\$/kWh
	Maximum WEC Spacing	$SPACE_{max}$	m

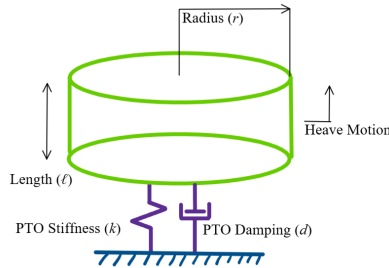


Figure 3: Schematic of the WEC geometry and control design variables.

The parameters for this problem are

$$\mathbf{p} = [\omega, A, \beta, i, \eta_{avail}, L, S, F_{max}, CAPEX_{med}] \quad (2)$$

where ω is the incoming wave frequency, A is the wave amplitude, β is the wave direction, i is the interest rate, η_{avail} is the wave availability coefficient, L is the anticipated WEC lifetime, S is the array scaling factor, F_{max} is the maximum force constraint on the PTO, and $CAPEX_{med}$ is the median capital cost as detailed in Section 2.5.

The following sections discuss each module in detail, including fundamental principles and equations as well as the optimization details, the sensitivity calculations and the discussion of the results.

2.1.1. Optimization

This study optimizes for two objectives using a multi-objective genetic algorithm (MOGA). A Pareto set is sought after to find the trade-off between the objectives. A non-dominated sorting genetic algorithm (NSGA-II) adapted for mixed variable types is used as an optimizer. NSGA-II is an evolutionary algorithm with elitist strategy, a parameter-less approach and efficient constraint-handling method (Deb et al. (2002)). We use a population size of 120 as well as the default hyperparameters utilized by the MixedVariableGA solver in the python library pymoo (Blank and Deb, 2020). Robust termination criteria in the objective function is used for the convergence. The tolerance level of 0.005 change in both objectives is required before the algorithm terminates.

2.2. Geometry and Layout

A heaving point absorber WEC is considered in this paper, and cost is directly related to its shape and size. Usually, the radius and draft are optimized for a wave environment. In addition to the optimal sizing of WECs, their layout is also important because how the WECs are situated will affect the wave field significantly. Such a design will also have to satisfy the competing requirement to minimize the ocean space used. Optimal dimensions for different layout types, such as a regular or staggered grid, are explored in literature (Yang et al., 2022). The fixing of the topology of the layout and only optimizing its dimension provides some computational benefits. Götteman et al. (2015) analyzed over 1000 interacting point absorbers using an approximate analytic method for single body diffraction. They found that among many different layouts (wedges, rectangle, circles, random) the

Table 2: Optimal geometry and PTO dampings for the different geometries shown in Fig. B.16.

Layout	Spacing [m]	r [m]	ℓ [m]	d_1 [$\frac{kNs}{m}$]	d_2 [$\frac{kNs}{m}$]	d_3 [$\frac{kNs}{m}$]	d_4 [$\frac{kNs}{m}$]
Grid	50	3	0.300	129	129	129	130
Grid	70	4	0.400	378	382	378	378
Line	30	4	0.400	414	446	451	421
Line	70	4	0.400	367	401	406	398

absorption power remains comparable, but the power variance differs significantly between configurations. This relation between power and layout could be vastly different if we were to include, for instance layout infrastructure costs, radiated waves and higher fidelity hydrodynamics analysis.

From the MDA perspective, the geometry module generates the WEC bodies on different locations as given by the optimizer. A heaving point absorber WEC is modeled as a simple cylinder (see Fig. 3) designed to float about its center of mass. The initial array layout and WEC positions are randomized to reduce influence on the heuristic optimization algorithm and find the most optimal conditions.

Our initial investigations show that WEC size and optimal PTO damping is dependent on array layout. We used a single objective heuristic optimization (with genetic algorithm) for LCOE finding the optimal geometry and control for WECs in two different layout types (grid and line, shown in Appendix Fig. B.16). The resulting optimal WEC geometry and dampings are shown in Table 2.

2.3. Hydrodynamics

Wave-structure interactions are commonly characterized using linear potential flow theory. The theory assumes the fluid velocity field \vec{v} is the gradient of some complex potential (ϕ), where $\vec{v} = \nabla\phi$ and ϕ satisfies the Laplace equation, $\nabla^2\phi = 0$. It also assumes inviscid, irrotational, and incompressible flow. $\phi(x, y, z)$ is complex velocity potential represented in $\Phi = \Re(\phi e^{-j\omega t})$

The boundary conditions for the associated boundary value problem (BVP) are

$$\begin{aligned}
\frac{\partial\phi}{\partial z}\Big|_{z=-h} &= 0 \\
\frac{\partial\phi}{\partial z} - \frac{\omega^2}{g}\phi\Big|_{z=0} &= 0 \\
\frac{\partial\phi}{\partial\vec{n}}\Big|_{\Gamma} &= \vec{u} \cdot \vec{n}
\end{aligned} \tag{3}$$

$$\lim_{R \rightarrow \infty} \left(\sqrt{kR} \frac{\partial\phi}{\partial R} - jk\phi \right) = 0$$

where $z = 0$ is the waterline, $z = -h$ is the sea floor, Γ is the body surface, \vec{n} is the normal vector to that surface, and \vec{u} is the body velocity and k is the wavenumber. This BVP is linearized by assuming a small wave steepness and small motion of the WECs around a mean position. Similarly, the hydrodynamics module also calculates the hydrostatic stiffness matrix of the WECs (C_{33}). For a stably floating body b a hydrodynamic analysis is then performed ($M_{bb} = \rho g V_b$). The density of sea water is ρ , g is acceleration due to gravity, V_b is the submerged volume of the WEC, and M_{bb} is the mass of the WEC.

Most common solvers modeling hydrodynamics are based on a reformulation of the governing PDE (Laplace equation) and associated boundary conditions as boundary integral equations (BIEs). These BIEs and the associated boundary element method (BEM) are well-suited for wave problems in unbounded domains and for complex geometries. In this method, only the body geometry is discretized into a mesh with panels and Green's identity is used to derive a boundary integral equation which is then discretized into a linear system. Thus, this method is ideal for design (size and shape) optimizations as only the body surface needs to be meshed. This is advantageous compared to meshing the domain (large ocean) around the floating body. This method is implemented in the open-source frequency-domain BEM code Capytaine (Ancellin and Dias (2019) Babarit and Delhommeau (2015)), our solver of choice.

When co-locating a system of interacting bodies, the energy produced when analyzed using linear potential flow theory may not linearly scale with the number of interacting bodies and has been shown to differ for various configurations from an isolated body (Budal (1977b)). The hydrodynamic interactions due to the superposition of diffracted and radiated waves from oscillating bodies can constructively or destructively affect the motion. These interactions are a function of WEC geometry and array configuration and affect wave power absorption of each body in the arrays. These interactions are important to consider in early design studies. Many different methods exist to simulate the array hydrodynamics such as analytical (Simon, 1982), semi-analytical (Zhong and Yeung (2016), McNatt et al. (2015), Singh and Babarit (2013)), predictive methods (Zhu et al., 2022), and full BEM resolution (interaction between all panels). Frequency domain BEM codes can solve the diffraction and radiation problems of wave-body interaction and calculate respective velocity potentials ($\phi_{\text{diffraction}}$, $\phi_{\text{radiation}}$), giving the total potential as

$$\phi_{\text{total}} = \phi_{\text{radiation}} + \phi_{\text{diffraction}} + \phi_{\text{incident}} \quad (4)$$

The wave elevation of the radiated, diffracted, and total wave fields is shown in Fig. 4, providing a visual for the wave-body interaction. The figure displays an arbitrary array of 4 WECs and how each component (radiation and diffraction) of the total potential for each WEC body impacts the surrounding wave field. Generally, the magnitude of radiated waves is slightly smaller than the diffracted waves, but both play a part in how the bodies oscillate.

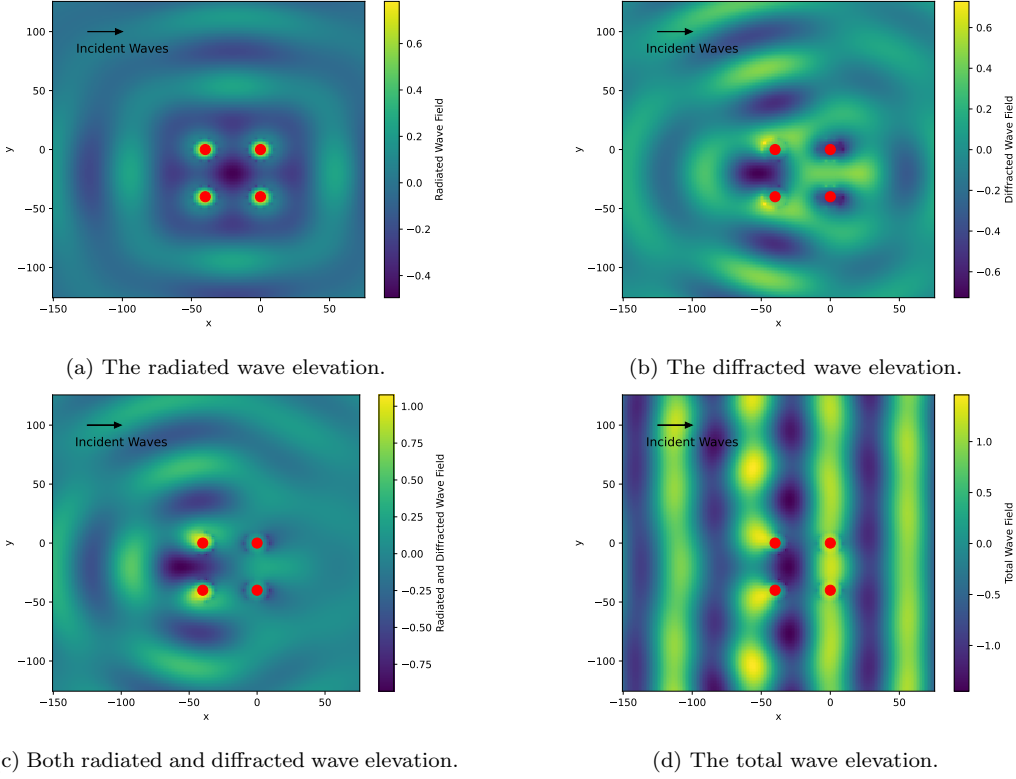


Figure 4: The elevation of the radiated, diffracted, and total wave fields for an arbitrary 4-body WEC array.

$\phi_{\text{radiation}}$ is used to calculate the hydrodynamic force coefficients $\mathbf{A}_{4 \times 4}$ and $\mathbf{B}_{4 \times 4}$ (added mass and damping in heave). Added mass (\mathbf{A}) and damping (\mathbf{B}) arise due to the motion of WECs. They are proportional to acceleration and velocity of the WEC respectively. They both depend on the wave frequency (ω). Heave excitation force ($\vec{F}_{1 \times 4}$) is found from the hydrodynamic pressure due to incident and scattered waves, the added mass, and the damping terms, described by

$$\vec{F} = -\omega\rho \int \int_{\Gamma} n_i \phi ds \quad (5)$$

$$\mathbf{A}_{ij} - \frac{j}{\omega} \mathbf{B}_{ij} = -\rho \int \int_{\Gamma} n_i \phi ds \quad (6)$$

where ω is the wave frequency, ρ is the fluid density, n_i is the normal vector, and ϕ is the potential.

2.3.1. Mesh Convergence

In order to ensure the accuracy of the coefficients, a mesh convergence study (see A.14) was done using few representative design obtained from Latin hypercube sampling ($N_S = 6$) of the design space. The mesh resolution for the analysis is shown in the Table 3.

Radius (r)	Resolution (nr, n θ , nx)
> 5	(7, 35, 25)
$4 < r \leq 5$	(5, 25, 20)
$3 < r \leq 4$	(3, 15, 15)
≤ 3	(2, 10, 10)

Table 3: Mesh resolution based on cylinder radius. nr, n θ , and nx represent the number of panels along a radius at the end, the number of panels around a slice, and the number of slices respectively.

Despite the high accuracy of full BEM resolution, researchers have been reluctant to use it for design optimization and sensitivity studies, mostly due to the computational limits. The direct numerical simulation has the computational cost of $O(N_p^2)$ for Green’s function evaluation and to setup the dense influence matrices and $O(N_p^3)$ for the solution of linear system, with N_p being the number of panels on all the WECs in an array. Free surface Greens function is also challenging to compute (Newman, 1985). Mesh convergence (see Fig. A.14) can be performed to reduce the number of panel required by only meshing to the required resolution (see Table 3). The computational cost and convergence of the BEM solvers also depends on the choice of linear solver and the dense influence matrix representation.

With integration of modern methods in the BEM codes, the computational cost can be somewhat reduced allowing for accurate designs and sensitivity studies to be affordable. The limitation has been removed to some extent by integrating many modern methods from BEM literature into marine hydrodynamic BEM solvers (Ancellin et al., 2024). Each block in the influence matrices is the interaction between a group of panels (as illustrated on Fig. 5). The interaction between distant blocks can be approximated by a low-rank matrix. Adaptive cross approximation (ACA) can be used to construct this low-rank matrix. The tolerance and distance for ACA are fixed to be 1e-1 and 7 \times radius, respectively.

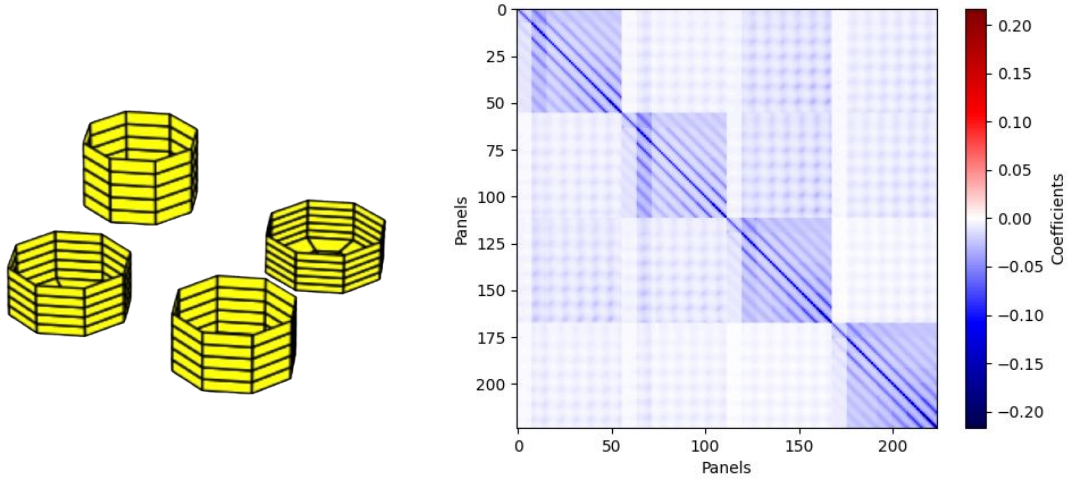


Figure 5: Block structure in influence matrices computed via full BEM resolution for any design.

Similarly, the boundary element solver has numerical issues such as irregular frequency and convergence issues. The removal techniques (Lee and Sclavounos, 1989) are not yet implemented in the open source numerical solver of choice - Capytaine. Thus, we add in a check to remedy this. A “sniff test” is implemented to disregard the ill-conditioned influence matrices ($\kappa(A) \geq 500$) to prevent the highly irregular added mass and damping coefficients. This is chosen based on our computational experiments although Newman suggests that BEM matrices build with free surface Greens function have condition number in $O(100)$ assuming high accuracy in Greens function calculation (Newman, 1985). If not accounted for, these can lead to erroneously high LCOE results. The genetic algorithm also avoids high LCOE results in its search for Pareto optimal designs. Any non-physical designs are further filtered during post processing.

2.4. Dynamics, Controls, and Power Take-Off

A simple controller commonly used in wave energy research is a reactive controller (Ringwood et al., 2014). Our WECs use a motor-actuated

reactive controller, and any WEC, i , uses the design variable PTO damping coefficient, d_i , and a model determined PTO stiffness term, k_i , as the two controller gains. These two controller gains are used in motor-actuated controllers to determine the force on the motor (F_{PTO}) as follows

$$F_{PTO} = k\xi + d\frac{\partial\xi}{\partial t} \quad (7)$$

where ξ is the heave motion of the WEC. For linear PTO devices, time-averaged power, P , for a given WEC, i , can be calculated with the following equation

$$P_i = \frac{1}{2}d_i|j\omega\mathbb{E}_i(j\omega)|^2 \quad (8)$$

where $\mathbb{E}_i(j\omega)$ is the complex amplitude of heave motion. Heave motion is assumed to be sinusoidal for each WEC, and oscillating at same frequency of the waves, ω . This allows the use of the following time domain equation

$$\xi_i = \mathbb{E}_i(j\omega)e^{-j\omega t} \quad (9)$$

where t represents the time variable and ξ_i is the time domain representation of heave motion. To calculate the complex amplitude of heave motion the coupled dynamics need to be solved.

$$\frac{\vec{\mathbb{E}}(j\omega)}{A} = [-\omega^2(\mathbf{M} + \mathbf{A}) - j\omega(\mathbf{B} + \text{diag}(\vec{d})) + \mathbf{C} + \text{diag}(\vec{k})]^{-1}\vec{\mathbb{F}}(j\omega) \quad (10)$$

The added mass matrix in heave (\mathbf{A}), hydrodynamic damping matrix in heave (\mathbf{B}), hydrostatic stiffness in heave (\mathbf{C}), and heave wave exciting force ($\vec{\mathbb{F}}(j\omega)$) all come from the hydro module. A is the wave amplitude parameter, \mathbf{M} is the diagonal array mass matrix, and $\text{diag}(\vec{d})$ forms a diagonal matrix using the values contained in the PTO damping vector. The components of the PTO stiffness vector (\vec{k}) are calculated to ensure decoupled resonance at the wave frequency ω using

$$k_i = \omega^2(M_{ii} + A_{ii}) - C_{ii} \quad (11)$$

where M_{ii} is the mass of WEC i .

Finally, the individual WECs power outputs are summed to obtain the total array power production.

2.4.1. Force Saturation

With unconstrained reactive controllers tuned to resonate, it is common to see unrealistic forces on the PTO. To properly consider controller design, it is important to both consider controller gains as well as constraints. For example, any realization of a motor actuated controller will have some maximum force. Using the heave motion calculated by Equation 10, the total unsaturated force on each PTO, $\mathbb{F}_{\text{PTO},i}(j\omega)$ can then be calculated using

$$\mathbb{F}_{\text{PTO},i}(j\omega) = \mathbb{E}_i(j\omega) \sqrt{k_i^2 + \omega^2 d_i^2} \quad (12)$$

If the magnitude of this force is larger than the maximum PTO force parameter, F_{max} , the response needs to be saturated. The method used to saturate the response is the same as the method used by McCabe et al. (2022). Using that method, a multiplier, μ_i , is found that modifies the PTO damping and stiffness for each WEC individually. If the magnitude of $\mathbb{F}_{\text{PTO},i}(j\omega)$ is less than or equal to F_{max} then μ_i is set to 1 for that WEC.

$$\begin{aligned} k_{i,sat} &= \mu_i k_i \\ d_{i,sat} &= \mu_i d_i \end{aligned} \quad (13)$$

These new saturated PTO gains can be used to recalculate motion ($\vec{\mathbb{E}}(j\omega)$) using Equation 10, with \vec{k}_{sat} and \vec{d}_{sat} substituted for \vec{k} and \vec{d} . This recalculated heave is then used in Equation 8 to calculate power.

It is worth noting that the force saturation model does not fully account for the coupling due to the array interactions. The motion of one WEC impacts the motion of all other WECs, meaning that performing the force saturation procedure on any one WEC the PTO force ($\mathbb{F}_{\text{PTO},i}(j\omega)$) changes for all the others. Another method for handling the force saturation that also fails to fully address coupling is to perform the saturation method one WEC at a time, recalculating the heave motion for all WECs after each saturation. A comparison of the results of these two methods (with F_{max} set to 10^5 N) is shown in Table 4. The table shows that there is minimal, 5%, difference between the two methods, and was used to justify the the force saturation method we used. Future work is required to fully capture the coupling effects in the force saturation model within the larger context of the multidisciplinary model.

2.4.2. Q-factor

We extend the discussion on the optimal average power with the q-factor. Q-factor (q) is commonly used to evaluate array power output. This metric

Table 4: Comparison of the two different force saturation modeling methods discussed. Method 1 is the method used in the study that saturates all the WECs at once. Method 2 saturates the WECs one at a time. The Balitsky column numbers come from an array like the one pictured in Fig. B.17 in the Appendix (Balitsky et al., 2018), and the diamond layouts are pictured in Fig. B.18 in the Appendix. The WECs used in the Balitsky layout have a radius of 5 m, length of 4 m, and damping coefficient of 3.6×10^5 Ns/m. The WECs used in the diamond layouts have a radius of 7 m, length of 0.7 m, and a damping coefficient of 5.01×10^5 Ns/m.

	Balitsky	Diamond (tight)	Diamond (spacious)
No Saturation	1328.2 kW	516.0 kW	970.5 kW
Method 1	507.9 kW	191.9 kW	150.3 kW
Method 2	505.9 kW	166.1 kW	135.4 kW
Saturation change	-62%	-63%	-85%
Method 2 change	-0%	-5%	-2%

is the ratio of the power produced by an array configuration of n bodies (P_{array}) to the power produced by n isolated bodies, shown by

$$q = \frac{P_{array}}{n \times P_{isolated}} \quad (14)$$

2.5. Economics

The economics module serves to compute the LCOE

$$\text{LCOE} = \frac{\text{CAPEX}_{ann} + \text{OPEX}}{\text{AEP}} \quad (15)$$

where CAPEX_{ann} is the annualized capital expenses, OPEX is the annual operating expenses, and AEP is the annual energy production. CAPEX_{ann} includes the cost of each WEC based on mass, the cost of the mooring lines, the installation cost, and the shipping costs. OPEX incorporates maintenance costs, mid-life refit costs, and decommissioning costs (all annualized). The median CAPEX_{ann} values and method for finding OPEX reported by the OES (Chozas (2015), Chang et al. (2018)) are used in this calculation and are scaled by the mass of the WEC

$$\text{xPEX} = \text{xPEX}_{med} + \left(\text{xPEX}_{med} * \frac{m}{m_{max}} \right) \quad (16)$$

where xPEX represents either CAPEX (pre-annualized) or OPEX and m_{max} is the mass of the largest WEC included in the OES report. The

reported xPEX values are normalized by the rated power, so they must be multiplied by the rated power of the corresponding WEC and then scaled by the modeled WECs. The median CAPEX value is taken directly from the EOS report as \$9000/kW, and the median OPEX is taken to be 5% of the median CAPEX, or \$450/kW. The CAPEX is annualized using

$$\text{CAPEX}_{ann} = \text{CAPEX} \frac{i(1+i)^L}{(1+i)^L - 1} \quad (17)$$

where i is the interest rate and L is the WEC lifetime. The annual energy production is calculated by

$$\text{AEP} = P \times \eta_{trans} \times \eta_{avail} \quad (18)$$

where η_{trans} and η_{avail} account for losses due to transmission lines and availability of wave power, respectively. This method effectively finds the ratio between WEC mass and mechanical power production and reports the corresponding economics metric.

3. Validation

The hydrodynamics and dynamics modules along with the power production were validated against another study involving arrays of cylindrical WECs (Balitsky et al. (2018)). The study analyzed the interactions between two clusters of WECs using coupled BEM and MILDwave model (MILDwave is a numerical wave propagation model). The layout of each cluster is shown in the Appendix in Fig. B.17. Each cylinder has a radius of 5 meters and a length of 4 meters, and uses resistive (meaning the PTO stiffness vector k is all zeros) control with each WEC having a PTO damping gain of 0.360 MNs/m. Note that this study also does not use force saturation so that is not included in this validation. The incoming waves ($\beta = 0$) are going from left to right with a period of 6 seconds and a unit amplitude. The two clusters are placed directly downstream from each other with three different spacings between clusters (500 m, 1000 m, 2000 m). A comparison is shown in Table 5. We see a maximum error of 1.55% between this model's results and the results of Balitsky et al.

Table 5: Comparison of model in this paper with results from Balitsky et al.

Cluster Spacing	Balitsky	This Paper	Error
500 m	1381 kW	1392 kW	+0.80%
1000 m	1682 kW	1707 kW	+1.55%
2000 m	1595 kW	1589 kW	-0.38%

4. Results

4.1. Pareto

The Pareto front, resulting from the optimization in Section 2.1.1 shown in Fig. 6, depicts the trade-off between minimizing farm length and minimizing LCOE. To reach the lowest LCOE, a larger amount of ocean space is required; however, a reasonable LCOE can still be achieved with a much smaller farm length with optimal radii, lengths, and damping coefficients. The lowest ocean space solution shows a 37% reduction in ocean space used compared to the minimized LCOE; with only a 5% increase in LCOE. The mean damping for the minimal LCOE design is 357 kNs/m, with a 0.0130 coefficient of variation. The mean damping for the minimal spacing design is 369 kNs/m, with a 0.0480 coefficient of variation. The minimized LCOE configuration can be seen in Fig. 8a, while the minimized farm length configuration can be seen in Fig. 8b. The distance between them vary depending on their size; designs that are compact tend to have higher LCOE values than designs spaced far enough apart such that interactions are negligible. The resulting rhombus-like configuration, at varying levels of compactness, is optimal for four WEC arrays in terms of minimizing both LCOE and ocean space. However, more compact configurations may require more individualized controls in order to reduce energy losses. Note that some of the designs found through the optimizer were removed in post processing due to the non-physical behavior predicted by our model. The pareto front with this points included can be found in the Appendix Fig. C.19.

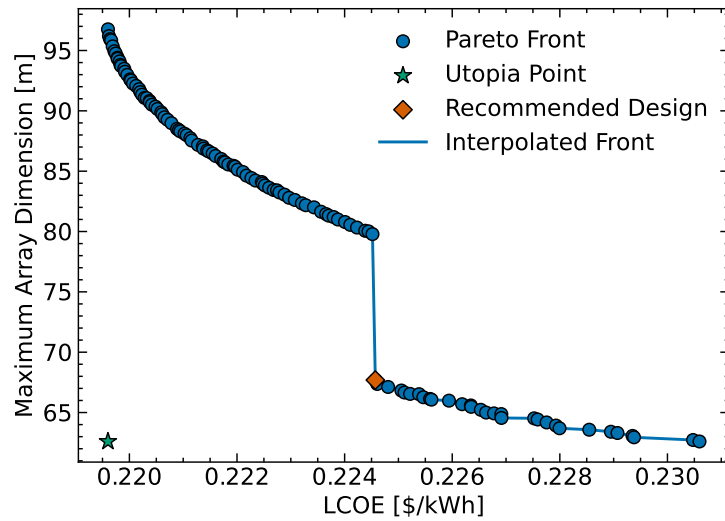


Figure 6: Pareto front generated by NSGA-II. A ‘recommended design’ (shown in Fig. 7) is highlighted for which further sensitivity analysis is performed. The decision space looks discretized across the pareto front.

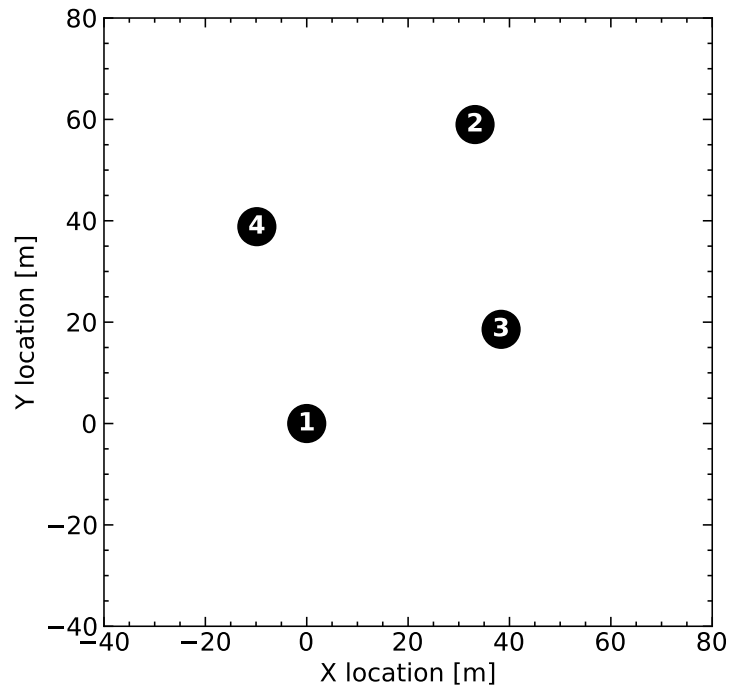


Figure 7: Recommended design

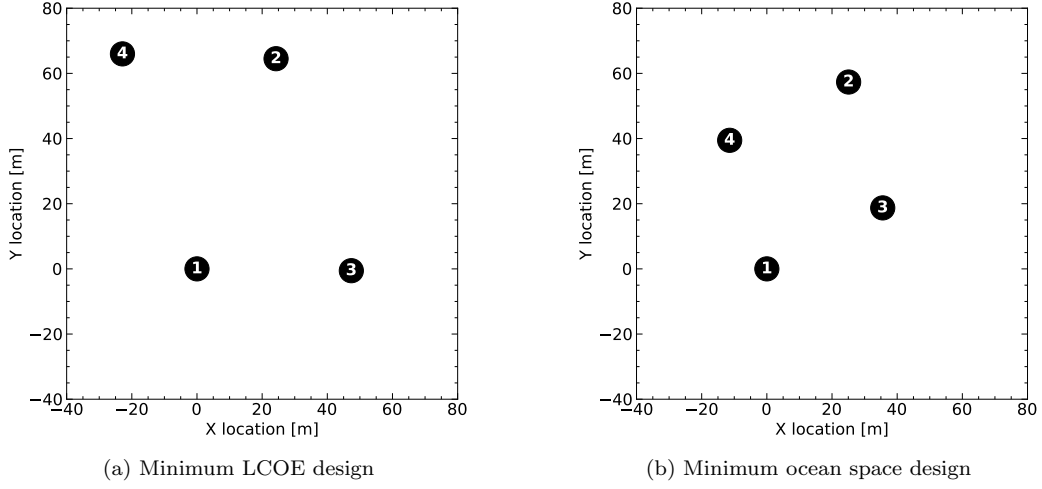


Figure 8: Minimum LCOE and ocean space designs from the Pareto front.

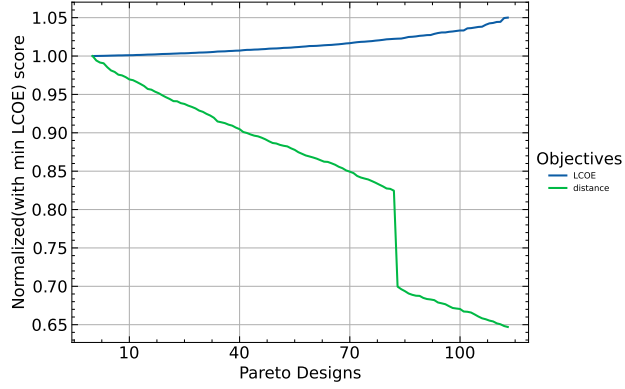


Figure 9: Change in the objectives across the pareto design normalized with min LCOE design

4.2. Disturbance Coefficients

The disturbance coefficient is the ratio of the total wave elevation (ζ_{total}) in the presence of WECs to the incident wave elevation (ζ_{inc}), defined as

$$k_d = \frac{\zeta_{total}}{\zeta_{inc}} \quad (19)$$

This ratio shows the magnitude of which the presence of the bodies affects the surrounding wave field. Fig. 10 shows the disturbance coefficient (k_d) for

the minimized LCOE and minimized farm length configurations. The higher k_d values in front of and to the side of the WECs indicate higher wave reflection from those bodies. The amount of wave height a WEC body can reflect directly relates to how much power they are able to extract from the waves. Additionally, the configuration of the WECs leads to higher reflections for each body due to the interaction effects. The magnitude of these reflections is comparable for both configurations; however, upstream of the minimized LCOE configuration exhibits more increased wave height overall. This indicates more synergistic effects than the minimized farm length configuration. In both configurations, WECs furthest from the incoming wave front experience shadowing effects, where the downstream wave height is not as great as upstream. However, these effects are minimal in our Pareto optimal solutions compared to a standard grid or un-optimized staggered layout.

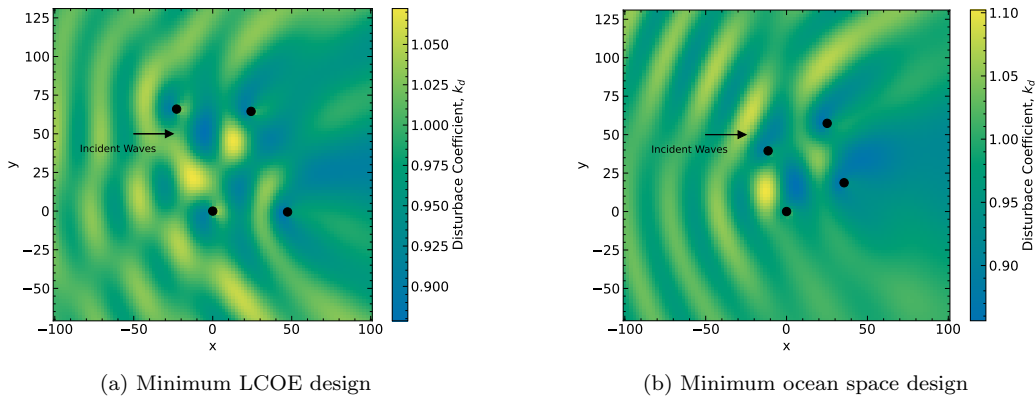


Figure 10: Disturbance coefficient (k_d) for the wave fields around two Pareto designs.

4.3. Q -Factors

The q -factors for the Pareto front designs are shown in Fig. 11a and 11b. Favorable q -factors are found for all designs, showing that these Pareto designs out-perform isolated WECs. The cluster on the Pareto front with the minimal LCOEs reach the highest q -factors, up to 1.06. This confirms the way the bodies interact in that specific configuration slightly magnifies the power production. The extent which the amplification is felt could potentially be under-predicted by mid fidelity model such as BEM, but still leads to solid array designs. The interaction of the fidelity of the model and controls parameters is a topic for future work.

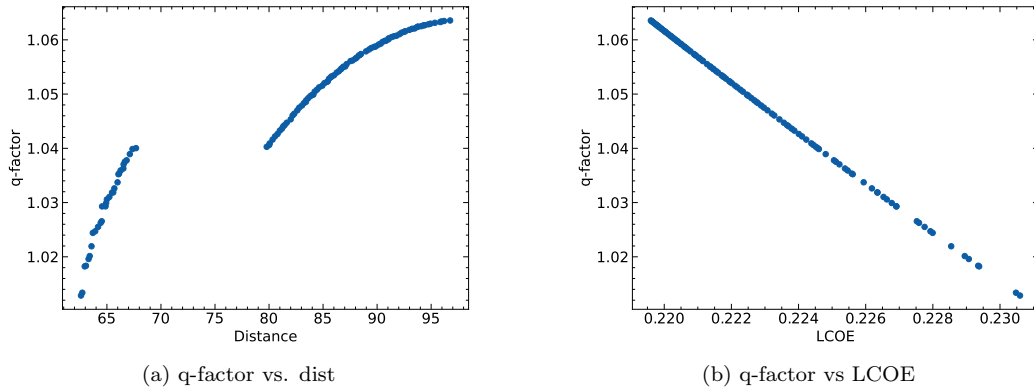


Figure 11: Variation of q-factor for each objective for the set of optimal designs

4.4. Ad-hoc Regression Model For Trade-off Analysis

The interaction of the objectives and design variables in the Pareto front are analysed for system level inferences. A simple regression model (see Fig. 12) is fitted for interpretability for the relation between the objectives (LCOE and distance) for the discrete decision space as shown by the Pareto front clusters (see Fig. 6). Analysis like this are essential to help facilitate the stakeholders and managers understand and interpret the results of multi-objective problems. Both models explain around 95% ($[0.95, 0.96]$) variation expected in the LCOE for optimal designs. The expected LCOE is shown by

$$LCOE_1 = 0.2475 - 0.0003 \times distance_1 \quad (20)$$

$$LCOE_2 = 0.3035 - 0.0012 \times distance_2 \quad (21)$$

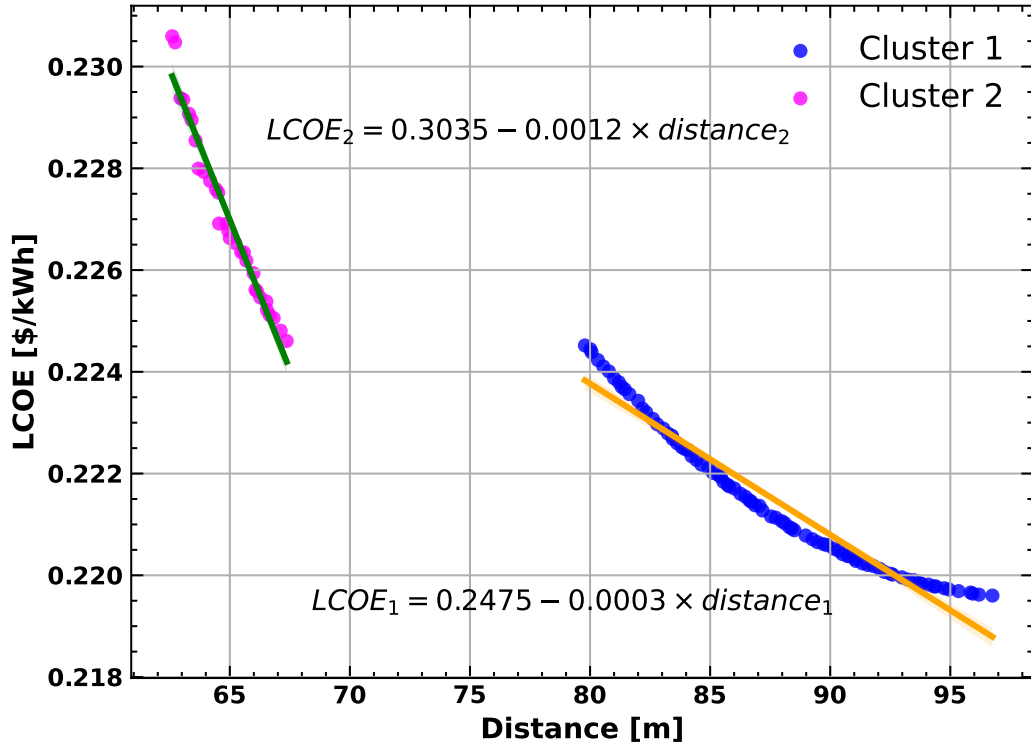


Figure 12: Different linear models for tradeoff analysis in discrete design space in the Pareto front from the multiobjective optimization.

The subscripts indicate clusters. 1 is the cluster with low LCOE and 2 is the cluster with low maximum array dimensions. The optimal (minimized) LCOE in compact layouts can be expected to decrease by $3e-4$ (\$/kWh) for every meter increase in the distance and by $1.2e-3$ (\$/kWh) for expanded arrays. The relationship in the larger layouts is not as linear as the decision in compact arrays. It is discussed here strictly for interpret-ability purposes rather than predictive purposes. This analysis is however not extensible to other optimization where the constraints, bounds and number of design variable are different.

5. Global Sensitivity Analysis

Sobol Sequence method is used to generate the samples using Python package SA-Lib (Wu (2017)) over a multi-dimension parameter space from different technical domain outlined in xDSM (see Fig. 1) diagram. The

goal is to fully capture the relationship between the unconditional variance of optimal WEC farm design to the variance of the dominant parameters in each of the involved disciplines. A convergence study is first performed to assess the required sampling size as the accuracy of this method depends the sample size. There is a limiting benefit to the sample size. Convergence around $N_{sobol} = 4000$ for total samples = $N_{sobol} \times (2D + 2)$ suggests that is good enough samples for sensitivity calculations for most parameters (see Fig. A.15). D being the total number of parameter inputs ($D = 7$) and using 1000 bootstrapping samples to get the average of the sensitivities.

Sobol variance decomposition method expresses the variation of the output as the superposition of the variation of the input. The total variance V of the model output Y can be decomposed as

$$V(Y) = \sum_{i=1}^d V_i + \sum_{i<j}^d V_{ij} + \dots + \sum_{i<j<k}^d V_{1\dots d} \quad (22)$$

where V_i is first-order or independent effect of the parameter, V_{ij} is second-order effect, and d is the total number of input parameters.

Sobol indices provide insights into the how the uncertainties of the input parameters and their interactions contributes to the variance of the output (minimized LCOE). For each parameter (X_i), the total Sobol index gives a measure of total influence on ($LCOE$) along with its interaction with other parameters (X_j). This allows for an assessment of the subsystems parameter interactions on the Pareto optimal designs. The total sensitivity of a design (ST) is

$$ST = 1 - \frac{V(E(Y|X_i))}{V(Y)} \quad (23)$$

The total sensitivity for a design in the Pareto set with design vector for recommended design (see Figs. 6 and 7).

Wave heading variance impacts about 10% of the total variance of LCOE suggesting accurately modeling wave heading in the hydrodynamic analysis of WEC farms increases the reliability. Wave heading being sensitive is expected because although a single point absorber WEC is axisymmetric, the array is not. Thus, designers aiming to reduce LCOE by 10% should try to reduce all variance of wave heading. Similarly, all others parameters with very small sensitivity index can be set at a constant value for the multi-disciplinary system analysis. This confirms with what is generally expected

Table 6: Parameter Bounds. All parameters are uniformly sampled in the bounds

Parameter	Description	Lower Bound	Upper Bound	Total Sensitivity
wave_heading	Wave Direction (rad)	$-\pi$	π	0.1
omega	Wave Frequency (rad/s)	0.1	3	0.04
L	WEC Lifetime (years)	5	35	3.0e-3
wave_amplitude	Amplitude of waves (m)	0.2	3	1e-2
interest	Interest rate (-)	0.05	0.2	3e-4
n_{avail}	Wave availability (-)	0.79	0.99	1.5e-4
S	Array Scaling Factor (-)	0.5	0.99	7.7e-5
F_{max}	Maximum saturation force (N)	1e4	1e6	1.5e-8

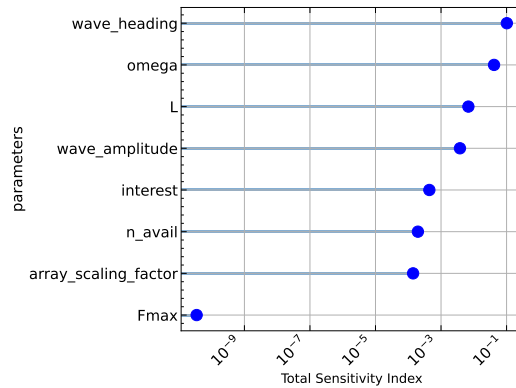


Figure 13: Total sensitivity (ST) of the optimal LCOE (design with LCOE = 0.21, distance = 53.5) to parameters. Omega, wave heading and draft seems to be sensitive to the LCOE.

for ‘linear’ models in each of the subsystem. From the multidisciplinary optimization point of view, we confirm the change in the wave environment, interest rate, and lifetime have some combined impact on the variability of the LCOE of the WEC farms. The viability of the WEC farm obtained here will differ by wave environment more than economics parameter probably due to simplified economics module adopted in this optimization. Note that the hydrodynamics solver here assumes a regular wave and the wave environment parameters are all assumed independent. This could be different for the analysis under irregular waves and correlated parameters. As illustrated in the Table 6, the low sensitivity indices indicate that the problem is more or less linear. This suggests for system level analysis and optimization, the inclusion of more constraints, higher fidelity of governing equations solvers in each of the coupled discipline is needed to fully account the variance in the LCOE and reduce the risk.

6. Future Work

For the future work, similar analysis for large number of WECs with variable fidelity of the governing equations ($R_i(\mathbf{x}, \mathbf{p}; \hat{u})$) should be included. It should be noted that the BEM computational cost increases with an increasing number of WECs, so there is a strong need to adopt modern BEM methods and efficient computational tools such as GPUs in the hydrodynamic analysis. The numerical issues in the existing open source solver such as convergence and irregular frequency also causes difficulties in the analysis and optimization. Mooring and transmission lines are not considered in the dynamics; however, future work should investigate the cost savings of sharing these lines, potentially making tighter configurations more favorable. Since this study only considers a single monochromatic wave, future studies should look at a JONSWAP spectrum or another similar spectrum that more accurately approximates a real sea-state. Not only should a frequency spectrum be considered in future work but, a spectrum of wave headings should also be considered. Additionally, an improved hydro module, or perhaps adding a feasibility constraint to match the solver fidelity, is necessary to prevent the optimizer from finding designs that lead to nonphysical results.

7. Conclusion

This paper details a multidisciplinary design optimization problem for WEC farms. A multidisciplinary analysis consisting of the array hydrodynamics, controls, and economics are discussed within this framework. For simplicity, only feed forward couplings were discussed. However, this framework can be extended to include the feedback coupling (for example, between mooring and hydrodynamics). A multi-objective genetic algorithm was used to analyze the relationship between competing objectives of minimizing farm length and minimizing LCOE. A sensitivity analysis of the Pareto optimal designs is conducted to evaluate their importance. The optimal rhombus-like configuration has varying levels of compactness as suggested by clusters in the Pareto fronts. This suggests there exists some configurations which are more ‘power dense’ than the others. The designs with these trade-off should be studied more. It is shown that the optimal LCOE (minimized) is sensitive to the variance in wave environments, mostly wave heading (β) and wave frequency (ω) thus providing information to designers on where to target to reduce risk (uncertainty). Similarly, a regression model is developed

to understand the trade-off between the two objectives for different decision space in the Pareto front.

This paper adopts a multidisciplinary systems analysis and optimization methodology to provide guidance to both WEC array designers and to the stakeholders regarding Pareto-optimal design heuristics, sensitivities, model calibration and uncertainty (risk) assessments. The analysis and the optimization code in this paper are open-source and can be accessed in the github: https://github.com/symbiotic-engineering/wec_array_opt.

8. CRediT authorship contribution statement

Kapil Khanal: Conceptualization, Methodology, Software, Formal analysis, Investigation, Data Curation, Original Draft, Review & Editing, Visualization. **Nate DeGoede:** Conceptualization, Methodology, Software, Validation, Writing - Review & Editing. **Olivia Vitale:** Conceptualization, Methodology, Writing - Review & Editing, Visualization. **Dr.Maha N Haji:** Resources, Supervision, Writing - Review & Editing, Funding acquisition

9. Acknowledgement

Authors would like to thank Carlos S. Michelen, Matthieu Ancellin, Rebecca McCabe and Matthew Haefner for their valuable feedback on the simulation and analysis in this manuscript. This work was supported in part by the Graduate Fellowship (for first year doctoral students) via Systems Engineering Department.

Appendix A. Convergence

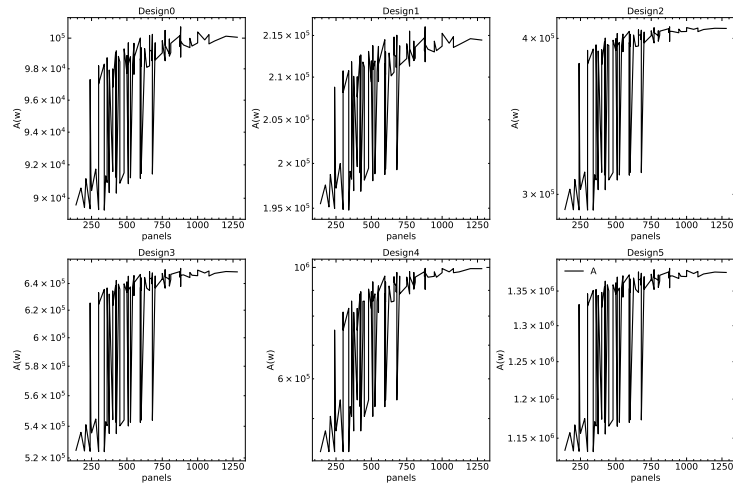


Figure A.14: Mesh convergence for sample designs. The number of panel is shown on the x-axis and the $A(\omega)$ is shown on the y-axis. All of these design converge for at least 750-1000 panels.

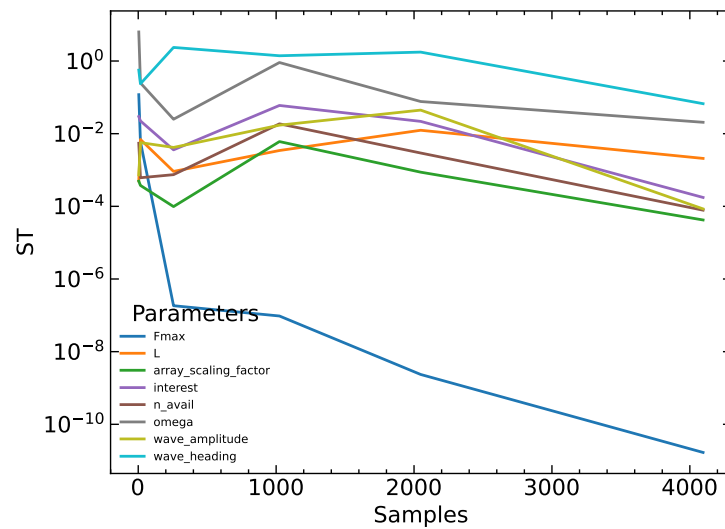


Figure A.15: Sobol convergence

Appendix B. Nominal Array Layouts

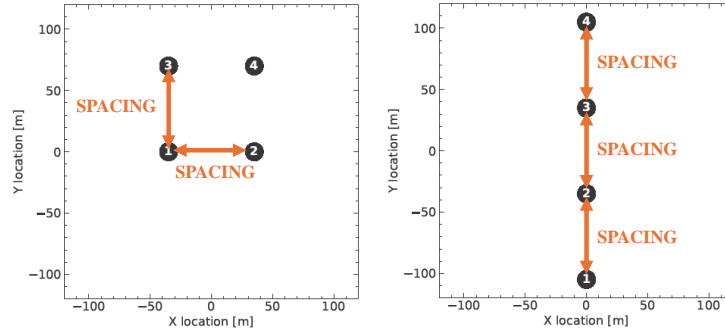


Figure B.16: Plots of nominal array layouts corresponding to the single objective optimization results in Table 2. The left corresponds to “grid” and the right is “line”.

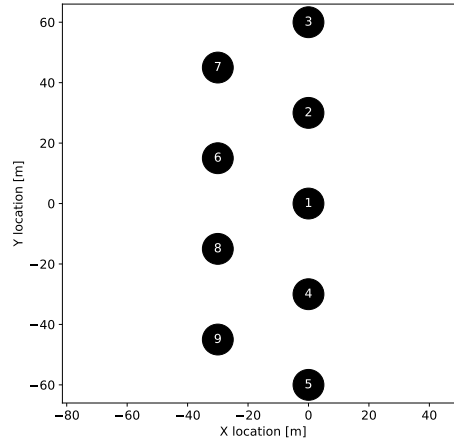


Figure B.17: Layout of one cluster from Balitsky study, used for validation.

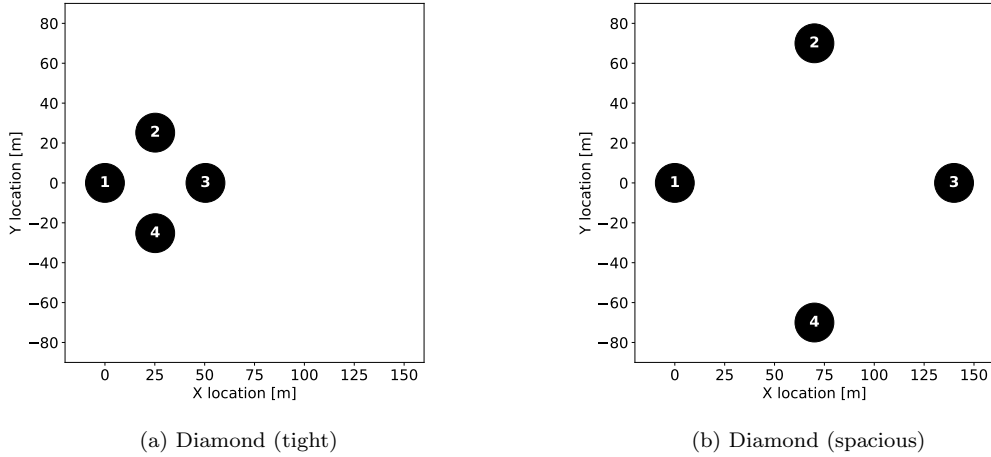


Figure B.18: Diamond layouts mentioned in Table 4.

Appendix C. Unfiltered Pareto

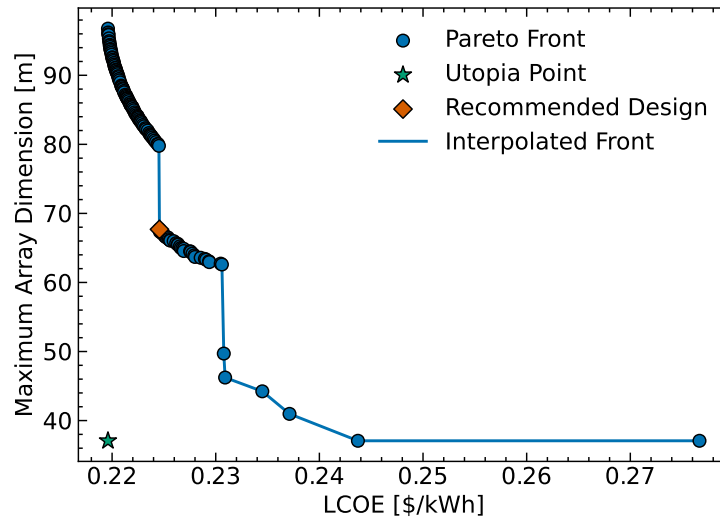


Figure C.19: Plot of the unfiltered Pareto front. The six points with the smallest Maximum Array Dimension are the points that got filtered.

References

Abdulkadir, H., Abdelkhalik, O., 2023. Optimization of heterogeneous arrays of wave energy converters. *Ocean Engineering* 272, 113818. URL: <https://>

- doi.org/10.1016/j.oceaneng.2023.113818, doi:10.1016/j.oceaneng.2023.113818.
- Ancellin, M., Dias, F., 2019. Capytaine: a Python-based linear potential flow solver. *Journal of Open Source Software* 4, 1341. URL: <https://doi.org/10.21105/joss.01341>, doi:10.21105/joss.01341.
- Ancellin, M., Marchand, P., Dias, F., 2024. Towards high-performance linear potential flow bem solver with low-rank compressions. *Energies* 17. URL: <https://doi.org/10.3390/en17020372>.
- Babarit, A., 2013. On the park effect in arrays of oscillating wave energy converters. *Renewable Energy* 58, 68–78. URL: <https://www.sciencedirect.com/science/article/pii/S096014811300164X>, doi:<https://doi.org/10.1016/j.renene.2013.03.008>.
- Babarit, A., Delhommeau, G., 2015. Theoretical and numerical aspects of the open source BEM solver NEMOH, in: *Proceedings of the 11th European Wave and Tidal Energy Conference (EWTEC2015)*, Nantes, France.
- Babarit, A., Hals, J., Muliawan, M., Kurniawan, A., Moan, T., Krokstad, J., 2012. Numerical benchmarking study of a selection of wave energy converters. *Renewable Energy* 41, 44–63.
- Balitsky, P., Verao Fernandez, G., Stratigaki, V., Troch, P., 2018. Assessment of the power output of a two-array clustered wec farm using a bem solver coupling and a wave-propagation model. *Energies* 11, 2907. doi:10.3390/en11112907.
- Blank, J., Deb, K., 2020. Pymoo: Multi-objective optimization in python. *IEEE Access* 8, 89497–89509. doi:10.1109/ACCESS.2020.2990567.
- Bozzi, S., Giassi, M., Moreno Miquel, A., Antonini, A., Bizzozero, F., Gruosso, G., Archetti, R., Passoni, G., 2017. Wave energy farm design in real wave climates: the italian offshore. *Energy* 122, 378–389. URL: <https://www.sciencedirect.com/science/article/pii/S0360544217301019>, doi:<https://doi.org/10.1016/j.energy.2017.01.094>.

- Budal, K., 1977a. Theory for absorption of wave power by a system of interacting bodies. *J Ship Res* 21, 248–254. URL: <https://doi.org/10.5957/jsr.1977.21.4.248>, doi:10.5957/jsr.1977.21.4.248.
- Budal, K., 1977b. Theory for absorption of wave power by a system of interacting bodies'. *Journal of Ship Research*, 21(04) URL: <https://doi.org/10.5957/jsr.1977.21.4.248>.
- Carta, J.A., Díaz, S., Castañeda, A., 2020. A global sensitivity analysis method applied to wind farm power output estimation models. *Applied Energy* 280, 115968. URL: <https://doi.org/10.1016/j.apenergy.2020.115968>, doi:10.1016/j.apenergy.2020.115968.
- Chang, G., Jones, C.A., Roberts, J.D., Neary, V.S., 2018. A comprehensive evaluation of factors affecting the levelized cost of wave energy conversion projects. *Renewable Energy* 127, 344–354. URL: <https://doi.org/10.1016/j.renene.2018.04.071>, doi:10.1016/j.renene.2018.04.071.
- Chozas, J., 2015. International levelised cost of energy for ocean energy technologies. *Ocean Energy Syst* .
- Cramer, K.J., Dennis Jr, J.E., Frank, P.D., Lewis, R.M., Shubin, G.R., 1994. Problem formulation for multidisciplinary optimization. *SIAM Journal on Optimization* 4, 754–776.
- de Andrés, A., Guanache, R., Meneses, L., Vidal, C., Losada, I., 2014. Factors that influence array layout on wave energy farms. *Ocean Engineering* 82, 32–41. URL: <https://www.sciencedirect.com/science/article/pii/S0029801814000651>, doi:<https://doi.org/10.1016/j.oceaneng.2014.02.027>.
- Deb, K., Pratap, A., Agarwal, S., Meyarivan, T., 2002. A fast and elitist multiobjective genetic algorithm: Nsga-ii. *IEEE Transactions on Evolutionary Computation* 6, 182–197. doi:10.1109/4235.996017.
- Ehler, C.N., 2021. Two decades of progress in marine spatial planning. *Marine Policy* 132, 104134. URL: <https://www.sciencedirect.com/science/article/pii/S0308597X18303816>, doi:<https://doi.org/10.1016/j.marpol.2020.104134>.

- Folley, M., Babarit, A., Child, B., Forehand, D., O'Boyle, L., Silverthorne, K., Spinneken, J., Stratigaki, V., Troch, P., 2012. A review of numerical modelling of wave energy converter arrays, in: Volume 7: Ocean Space Utilization; Ocean Renewable Energy. International Conference on Off-shore Mechanics and Arctic Engineering. doi:<https://doi.org/10.1115/OMAE2012-83807>.
- Freeman, M.C., O'Neil, R., Garavelli, L., Hellin, D., Klure, J., 2022. Case study on the novel permitting and authorization of pacwave south, a us grid-connected wave energy test facility: Development, challenges, and insights. *Energy Policy* 168, 113141. doi:<https://doi.org/10.1016/j.enpol.2022.113141>.
- Galparsoro, I., Korta, M., Subirana, I., Borja, Á., Menchaca, I., Solaun, O., Muxika, I., Iglesias, G., Bald, J., 2021. A new framework and tool for ecological risk assessment of wave energy converters projects. *Renewable and Sustainable Energy Reviews* 151, 111539.
- Götteman, M., Engström, J., Eriksson, M., Isberg, J., 2015. Optimizing wave energy parks with over 1000 interacting point-absorbers using an approximate analytical method. Department of Engineering Sciences, Uppsala University, Sweden 10. doi:10.1016/j.ijome.2015.02.001.
- Kilcher, L., Fogarty, M., Lawson, M., 2021. Marine Energy in the United States: An Overview of Opportunities. Tech. Rep. NREL/TP-5700-78773. NREL. URL: <https://www.osti.gov/servlets/purl/1766861/>, doi:10.2172/1766861.
- Lambe, A.B., Martins, J.R.R.A., 2012. Extensions to the design structure matrix for the description of multidisciplinary design, analysis, and optimization processes. *Structural and Multidisciplinary Optimization* 46, 273–284. URL: <https://doi.org/10.1007/s00158-012-0763-y>, doi:10.1007/s00158-012-0763-y.
- Lee, C.H., Sclavounos, P.D., 1989. Removing the irregular frequencies from integral equations in wave-body interactions. *J. Fluid Mech.* 207, 393–418.
- Lyu, J., Abdelkhalik, O., Gauchia, L., 2019. Optimization of dimensions and layout of an array of wave energy converters. *Ocean Engineering* 192, 106543. URL: <https://www.sciencedirect.com/science/article/>

- pii/S0029801819306778, doi:<https://doi.org/10.1016/j.oceaneng.2019.106543>.
- Martins, J.R.R.A., Ning, A., 2022. Engineering Design Optimization. Cambridge University Press, Cambridge, UK. URL: <https://mdobook.github.io>, doi:10.1017/9781108980647.
- McCabe, R., Murphy, O., Haji, M., 2022. Multidisciplinary Optimization to Reduce Cost and Power Variation of a Wave Energy Converter Volume 3A: 48th Design Automation Conference (DAC). doi:<https://doi.org/10.1115/DETC2022-90227>.
- McNatt, J.C., Venugopal, V., Forehand, D., 2015. A novel method for deriving the diffraction transfer matrix and its application to multi-body interactions in water waves. *Ocean Engineering* 94, 173–185. doi:<https://doi.org/10.1016/j.oceaneng.2014.11.029>.
- Nahvi, Ali, 2018. Levelized cost of energy (lcoe) analysis of hexcrete wind towers doi:10.31224/osf.io/puw4q.
- Newman, J., 1985. Algorithms for the free-surface green function. *Journal of Engineering Mathematics* 19, 57–67. URL: <https://doi.org/10.1007/BF00055041>, doi:10.1007/BF00055041.
- Peña-Sanchez, Y., García-Violini, D., Ringwood, J.V., 2022. Control co-design of power take-off parameters for wave energy systems. *IFAC-PapersOnLine* 55, 311–316. URL: <https://www.sciencedirect.com/science/article/pii/S2405896322025848>, doi:<https://doi.org/10.1016/j.ifacol.2022.10.531>. 9th IFAC Symposium on Mechatronic Systems MECHATRONICS 2022.
- Ringwood, J.V., Bacelli, G., Fusco, F., 2014. Control of wave-energy converters. *IEEE Control Systems* , 30–55doi:10.1109/MCS.2014.2333253.
- Roberts, J.D., Bull, D.L., Costello, R.P., Babarit, A., Nielsen, K., Ferreira, C.B., Kennedy, B., Malins, R.J., Dykes, K., Weber, J., . Systems engineering applied to the development of a wave energy farm. URL: <https://www.osti.gov/biblio/1365534>, doi:10.2172/1365534.
- Saltelli, A., Andres, T., Homma, T., 1993. Sensitivity analysis of model output: An investigation of new techniques. *Computational Statistics & Data*

- Analysis 15, 211–238. URL: [https://doi.org/10.1016/0167-9473\(93\)90193-W](https://doi.org/10.1016/0167-9473(93)90193-W), doi:10.1016/0167-9473(93)90193-W.
- Sharp, C., DuPont, B., 2018. Wave energy converter array optimization: A genetic algorithm approach and minimum separation distance study. *Ocean Engineering* 163, 148–156. URL: <https://doi.org/10.1016/j.oceaneng.2018.05.071>, doi:10.1016/j.oceaneng.2018.05.071.
- Simon, M., 1982. Multiple scattering in arrays of axisymmetric wave-energy devices. part 1. a matrix method using a plane-wave approximation. *Journal of Fluid Mechanics* 120, 1–25. doi:10.1017/S002211208200264X.
- Singh, J., Babarit, A., 2013. Hydrodynamic interactions in multiple body array: a simple and fast approach coupling boundary element method and plane wave approximation, in: 32nd International Conference on Ocean, Offshore and Arctic Engineering (OMAE2013), Nantes, France. URL: <https://hal.archives-ouvertes.fr/hal-01201935>, doi:10.1115/OMAE2013-10541.
- Singh, J., Babarit, A., 2014. A fast approach coupling boundary element method and plane wave approximation for wave interaction analysis in sparse arrays of wave energy converters. *Ocean Engineering* 85, 12–20. URL: <https://www.sciencedirect.com/science/article/pii/S0029801814001589>, doi:<https://doi.org/10.1016/j.oceaneng.2014.04.019>.
- Sinha, A., Karmakar, D., Guedes Soares, C., 2016. Performance of optimally tuned arrays of heaving point absorbers. *Renewable Energy* doi:<https://doi.org/10.1016/j.renene.2016.02.043>.
- Wu, J.H., 2017. Salib: An open-source python library for sensitivity analysis. *Journal of Open Source Software* 2.
- Yang, B., Wu, S., Zhang, H., Liu, B., Shu, H., Shan, J., Ren, Y., Yao, W., 2022. Wave energy converter array layout optimization: A critical and comprehensive overview. *Renewable and Sustainable Energy Reviews* 167, 112668. URL: <https://www.sciencedirect.com/science/article/pii/S1364032122005603>, doi:<https://doi.org/10.1016/j.rser.2022.112668>.

- Zhong, Q., Yeung, R., 2016. Wave-body interactions among an array of truncated vertical cylinders, in: Proceedings of the ASME 2016 35th International Conference on Ocean, Offshore and Arctic Engineering, ASME, Busan, South Korea. p. V007T06A069. doi:10.1115/OMAE2016-55055.
- Zhu, K., Shi, H., Han, M., Cao, F., 2022. Layout study of wave energy converter arrays by an artificial neural network and adaptive genetic algorithm. *Ocean Engineering* 260, 112072. URL: <https://www.sciencedirect.com/science/article/pii/S0029801822014007>, doi:<https://doi.org/10.1016/j.oceaneng.2022.112072>.